JPET Fast Forward. Published on November 3, 2004 as DOI: 10.1124/jpet.104.077230

YC-1 Exhibits a Novel Antiproliferative Effect and Arrests the Cell Cycle in G0-G1 in Human Hepatocellular Carcinoma Cells

Shih-Wei Wang, Shiow-Lin Pan, Jih-Hwa Guh, Hui-Ling Chen, Dong-Ming Huang, Ya-Ling Chang, Sheng-Chu Kuo, Fang-Yu Lee, and Che-Ming Teng

Pharmacological Institute (S.W.W., S.L.P., D.M.H, Y.L.C., C.M.T.) and School of Pharmacy (J.H.G.), College of Medicine, National Taiwan University, Taipei, Taiwan; Hepatitis Research Center, National Taiwan University Hospital, Taipei, Taiwan (H.L.C.); Graduate Institute of Pharmaceutical Chemistry, China Medical University, Taichung, Taiwan (S.C.K.); and Yung-Shin Pharmaceutical Industry Co, Ltd, Taichung, Taiwan (F.Y.L.)

Running title : YC-1's antiproliferative activity in HCC

Corresponding author : Che-Ming Teng, Ph.D., Pharmacological Institutes, College of Medicine, National Taiwan University, No. 1, Jen-Ai Road, Sect. 1, Taipei, Taiwan.

TEL and FAX: 886-2-2322-1742; E-mail: cmteng@ha.mc.ntu.edu.tw

Number of text pages: 33

Number of tables: 1

Number of figures: 8

Number of references: 40

Number of words in Abstract: 217

Number of words in Introduction: 565

Number of words in Discussion: 1127

ABBREVIATIONS : HCC, hepatocellular carcinoma; YC-1, 3-(5'-hydroxymethyl-2'-furyl)-1-benzyl indazole; CDK, cyclin-dependent kinase; CKI, cyclin-dependent kinase inhibitor; sGC, soluble guanylyl cyclase; HIF-1, hypoxia-inducible factor-1; SRB, sulforhodamine B; DAPI, 4,6-diamidino-2-phenylindole; TUNEL, terminal deoxynucleotidyl transferase dUTP-biotin nick-end labeling; PAGE, polyacrylamide gel electrophoresis; DAB, diaminobenzidine; ODQ, 1*H*-(1,2,4)oxadiazolo(4,3-*a*)quinoxalin-1-one; KT5823, (8*R*,9*S*,11*S*)-(-)-2-methyl-9-methoxy-9-methoxycarbonyl-8-methyl-2,3,9,10-tetrahydro-8,11-epoxy-1*H*,8*H*,11*H*-2,7*b*,11*a*-triazadibenzo(*a*,*g*)cyclocta(*cde*)trinen-1-one; PD98059**,** 2'-amino-3'-methoxyflavone; LY294002, 2-(4-morpholinyl)-8-phenyl-1(4*H*)-benzopyran-4-one hydrochloride; MAPK, mitogen-activated protein kinase; PI3K, phosphatidylinositol 3-kinase.

JPET Fast Forward. Published on November 3, 2004 as DOI: 10.1124/jpet.104.077230
This article has not been copyedited and formatted. The final version may differ from this version.

ABSTRACT

This study delineates the antiproliferative activities and *in vivo* efficacy of YC-1 in human hepatocellular carcinoma (HCC) cells. YC-1 inhibited the growth of HA22T and Hep3B cells in a concentration-dependent manner without significant cytotoxicity. YC-1 induced G1 phase arrest in the cell cycle, as detected by an increase in the proportion of cells in G1 phase using FACScan flow cytometric analysis. It was further shown that neither cGMP, p42/p44 mitogen-activated protein kinase, nor AKT kinase-mediated signaling pathways contributed to the YC-1-induced effect. Of note, YC-1 induced a dramatic increase in the expression of cyclin-dependent kinase (CDK)-inhibitory protein, $p21^{CIP1/WAP1}$ and a modest increase in $p27^{KIP1}$. The association of $p21^{CIP1/WAP1}$ with CDK2 was markedly increased in cells responsive to YC-1. YC-1 did not modify the expression of cyclin D1, cyclin E, CDK2, or CDK4. In a corollary *in vivo* study, YC-1 induced dose-dependent inhibition of tumor growth in mice inoculated with HA22T cells. Immunohistochemical analysis revealed an inverse relationship between the staining of $p21^{CIP1/WAF}$ and the staining of Ki-67, a cell proliferation marker. Based on the results reported herein, we suggest that YC-1 induces cell cycle arrest and inhibits tumor growth both *in vitro* and *in vivo* via the up-regulation of $p21^{CIP1/WAP1}$ expression in HA22T cells. Because of this, YC-1 is a potential anti-tumor agent worthy of further investigation.

JPET Fast Forward. Published on November 3, 2004 as DOI: 10.1124/jpet.104.077230
This article has not been copyedited and formatted. The final version may differ from this version.

INTRODUCTION

Hepatocellular carcinoma (HCC) is one of the most common malignancies, ranking as the fifth leading cause of cancer mortality in the world (Parkin et al., 1999). Although most HCC cases occur in Eastern Asia and West Africa, the incidence has been increasing in the United States and other developed countries (El-Serag and Mason, 1999; El-Serag, 2002). To date, there are few promising therapeutic agents for the treatment of HCC because the disease is not very susceptible to currently available chemotherapeutic agents, which are also poorly tolerated by HCC patients. Therefore, there is an enormous need to develop effective chemotherapeutic agents with an acceptable side effect profile.

Uncontrolled cell proliferation or deregulated suppression of cell death permits neoplastic progression. Cytotoxic drugs have traditionally been the mainstay of chemotherapeutic approaches to treating cancers (Gibbs, 2000) but recently many studies have focused on the development of non-cytotoxic agents. This class of agents shows a “cytostatic” profile that affects the checkpoint of the cell cycle progression and inhibits tumor growth without direct cytotoxic insult to cancer cells (Owa et al., 2001; Millar and Lynch, 2003).

Tumor cells undergo uncontrolled proliferation by evading growth quiescence, which can be attributed to increased mitogenic signaling and/or alterations that lower the threshold required for cell-cycle progression (Elledge, 1996; Sherr, 2000). Deregulation of cell cycle progression is a hallmark of neoplasia (Malumbres and Barbacid, 2001). Eukaryotic cell

JPET Fast Forward. Published on November 3, 2004 as DOI: 10.1124/jpet.104.077230
This article has not been copyedited and formatted. The final version may differ from this version.

cycle progression is regulated by cyclin-dependent kinases (CDKs), which phosphorylate and dephosphorylate binding proteins such as cyclins and CDK inhibitors (CKIs) (Morgan, 1995). CDK protein levels remain stable, while cyclin levels vary in a way that periodically activates CDK during the cell cycle (Pines, 1991). In mammalian cells, cyclin D-CDK4/6 complex acts primarily in early G1 phase, cyclin E–CDK2 complex in middle-to-late G1 phase, and cyclin A-CDK2 complex in S phase (Stewart et al., 2003). The activation of cyclin-CDK complex can be inhibited by phosphorylation of a conserved threonine-tyrosine pair in CDK or by association with CKIs (Elledge, 1996). Two families of CKIs have been discovered, the Cip/Kip family and the INK4 family (Vidal and Koff, 2000). The Cip/Kip family, including $p21^{Cip1/Waf1}$, $p27^{Kip1}$ and $p57^{Kip2}$ which inhibit CDK2- and CDK4/6-cyclin complexes, is involved in G1 and G1/S regulation (Polyak et al., 1994; Harper et al., 1995; Lee et al., 1995). The INK4 family consists of $p16^{INK4a}$, $p15^{INK4b}$, $p18^{INK4c}$, and $p19^{INK4d}$, which narrow specifically to form stale complexes with CDK4/6 before binding with cyclinD (Vidal and Koff, 2000). In cancer cells, the signaling pathway involving CKIs is frequently disrupted, which leads to uncontrolled proliferation. Much evidence suggests that increased $p21^{Cip1/Waf1}$ and $p27^{Kip1}$ expression can inhibit the growth of various tumor types through the induction of G1 arrest in the cell cycle (Harper and Elledge, 1996).

YC-1 has been identified in our laboratory as an effective antiplatelet agent which increases cGMP levels through NO-independent activation of soluble guanylyl cyclase (sGC) (Wu et

al., 1995). Most of the actions of YC-1 in the cardiovascular system result in cGMP-dependent responses (Mulsch et al., 1997; Pan et al., 2004). Recently, YC-1 has been shown to inhibit the proliferation of vascular smooth muscle cells and endothelial cells (Hsu et al., 2003; Wu et al., 2004) and block tumor angiogenesis by suppressing hypoxia-inducible factor-1 (HIF-1) activity (Yeo et al., 2003). In the current study, we investigated whether YC-1 can directly affect cancer cell survival and growth and YC-1's anticancer mechanism in human HCC.

JPET Fast Forward. Published on November 3, 2004 as DOI: 10.1124/jpet.104.077230
This article has not been copyedited and formatted. The final version may differ from this version.

Materials and Methods

Cell Culture. The human hepatocellular carcinoma cell line HA22T (Culture Collection & Research Center, Taiwan) and Hep3B (American Type Culture Collection, USA) were cultured in Dulbecco's modified Eagle's medium (DMEM) (GIBCO BRL, Grand Island, NY) supplemented with 10% fetal bovine serum (FBS); penicillin (100 units/ml) and streptomycin (100 μg/ml) at 37°C in humidified air containing 5% CO_2.

Cell Growth Assay. Growth inhibition by YC-1 was measured using the sulforhodamine B (SRB) assay. YC-1 was added at a range of concentration alone or combined with several agents for 48 h. Cells were fixed with 50% TCA to terminate reaction, and 0.4% SRB (Sigma, St. Louis, MO) in 1% acetic acid was added to each well. After a 15-min incubation, the plates were washed, and dye were dissolved by 10 mM Tris buffer. Then the 96-well plate was read by enzyme-linked immunosorbent assay (ELISA) reader (515 nm) to get the absorbance density values.

[^{3}H]Thymidine Incorporation Assay. Cells were incubated without or with indicated reagents for 48 h. Before the harvest, cells were incubated with [^{3}H]thymidine (1 μCi/ml) for 16 h and then processed and harvested with Filter-Mate (Packard, Meriden, CT), and incorporated radioactivity was determined.

Cell Viability and Cytotoxicity Assay. Cells were incubated with vehicle (dimethyl sulfoxide), YC-1 (50 μM), and doxorubicin (3 μM) for 48 h. Both attached and floating cells

JPET Fast Forward. Published on November 3, 2004 as DOI: 10.1124/jpet.104.077230
This article has not been copyedited and formatted. The final version may differ from this version.

were collected by trypsinization and counted in duplicate by using hemocytometer. Trypan blue dye exclusion was used to determine viability. Cytotoxicity in cells was quantitated by measurement of lactate dehydrogenase (LDH). After lysis, the plate was read by ELISA reader to record absorbance at 490 nm.

Identification of Apoptosis. For the staining of apoptotic cells, the fluorescent DNA-staining dye, DAPI (Roche Molecular Biochemicals, Mannheim, Germany), was used to evaluate nuclear morphology and analyzed using ZEISS Axiovert 100TV microscope. In a parallel experiment, a terminal deoxynucleotidyl transferase (TdT) dUTP nick-end labeling (TUNEL) method was performed using an apoptotic detection kit (Promega, Madison, WI) and photomicrographs were obtained with a fluorescence microscope (Zeiss Axioskop 2 Microscope).

Cell Cycle Analysis. Following drug treatment, cells were harvested by trypsinization, washed with PBS, then pellets were resuspended and fixed in ethanol (70%, v/v). The cell cycle distribution was determined using FACScan flow cytometric analysis by DNA staining with propidium iodide and analyzed by CellQuest software (Becton Dickinson, Bedford, MA).

Assay of cGMP Contents. cGMP contents were assayed using enzyme immunoassay kits (Amersham Pharmacia Biotech, Buckinghamshire, UK). At confluence, monolayer cells were incubated with YC-1 for 15 min. Then, cells were washed twice with ice-cold PBS and lysed

JPET Fast Forward. Published on November 3, 2004 as DOI: 10.1124/jpet.104.077230
This article has not been copyedited and formatted. The final version may differ from this version.

with 0.5 ml NaOH (0.1 M). A 0.5 ml HCl (0.1 M) was then added to neutralize the assay solution. For the cGMP determinations, samples were acetylated. The assay was performed according to the manufacturer's instructions.

Western Blot Analysis. After the exposure of cells to the indicated agents and time courses, and reaction was terminated by the addition of lysis buffer (10 mM Tris–HCl, pH 7.4, 150 mM NaCl, 1 mM EGTA, 0.5 mM phenylmethylsulfonyl fluoride (PMSF), 10 μg/ml aprotinin, 10 μg/ml leupeptin, and 1% Triton X-100). The cell lysates were electrophoresized on 10–15% SDS-PAGE. The primary antibodies used in this study were ordered from Santa Cruz Biotechnology, except for Erk & Akt (Cell Signaling Technology, Beverly, MA), phosphorylated Erk & Akt (Cell Signaling Technology), cyclin D1 & α-tubulin (Oncogene Research Products, Cambridge, MA), p27 (BD Biosciences, Palo Alto, CA). Horseradish peroxidase-conjugated secondary antibodies (Santa Cruz Biotechnology, Santa Cruz, CA) were used, and the detection of signal was performed with an enhanced chemiluminescence detection kit (Amersham Pharmacia Biotech).

Immunoprecipitation. Total cellular proteins was immunoprecipitated with anti-CDK2 or CDK4 antibody and was mixed overnight at 4℃. The following day, 20 μg of protein A/G PLUS-Agarose (Santa Cruz Biotechnology) beads were added and incubated with gentle rocking for 1-3 h at 4℃. Immunoblotting was performed using anti-p21 antibody and anti-p27 antibody.

JPET Fast Forward. Published on November 3, 2004 as DOI: 10.1124/jpet.104.077230
This article has not been copyedited and formatted. The final version may differ from this version.

Tumor Xenografts Implantation. Male SCID mice (20 g, 4 weeks of ages), were obtained from Laboratory Animal Center of Medical College, National Taiwan University, and acclimated to laboratory conditions 1 week before tumor implantation. SCID mice were maintained in accordance with the Institutional Animal Care and Use Committee procedures and guidelines. HA22T cells (6×10^6 cells) injected s.c. into the flank of each animal. When tumors reached an approximate volume of 60 mm^3, mice bearing tumors with acceptable morphology and of similar size range were selected and distributed for drug studies. HA22T tumors were measured every 4 days using a caliper, and the body weights of the mice were monitored for toxicity. Tumor volumes were determined by measuring the length (l) and the width (w), and the volumes were calculated ($V=lw^2/2$). The mice were sacrificed when the tumor burden reached approximately 10% of total body weight and excised tumors were weighted.

Immunohistochemistry. Immunohistochemical studies were performed on formalin-fixed, paraffin-embedded tissue section of HA22T-induced tumor in SCID mice using streptavidin-biotin-peroxidase method by HRP-DAB system staining kit (R&D Systems, Minneapolis, MN). The primary antibodies : Ki-67 (MM1 ; Novocastra Laboratories, Newcastle upon Tyne, UK), p21 (DC360 ; Cell Signaling Technology), and p27 (C-19 ; Santa Cruz Biotechnology) were used in this study. The same protocol was carried out for negative controls, in which either the primary antibody was omitted or an isotype-matched control

antibody was used.

All slides were reviewed independently by 3 investigators and only those cells with nuclear reactivity were considered positive. At least 20 randomly selected high-power field with a minimum of 4000 cells were evaluated and scored in each slide. Ki67 and p21 staining were assessed quantitatively by counting the total number of positively stained nuclei per high-power field microscopically in the tumor. For the image cytometric analysis was performed with Image-Pro Plus.

Statistical analysis. Data are presented as the mean ± S.E.M. for the indicated number of separate experiment. Statistical analysis of data was performed with one-way analysis of variance (ANOVA) followed by a *t*-test and *p*-values less than 0.05 were considered significant.

JPET Fast Forward. Published on November 3, 2004 as DOI: 10.1124/jpet.104.077230
This article has not been copyedited and formatted. The final version may differ from this version.

Results

YC-1 Induces an Inhibitory Effect of Cell Growth in Human HCC Cells. YC-1 exerted a concentration-dependent inhibition of cell growth in HA22T and Hep3B cells, with an IC_{50} value of 46.1±4.0 μM and 47.2±1.9 μM, respectively (Fig. 1A). To independently evaluate this conclusion, a [^{3}H]thymidine incorporation assay was performed, yielding remarkably similar data with an IC50 value of 43.0±8.1 μM in HA22T cells (Fig. 1B).

YC-1 Induces a Cytostatic Effect via G1 Arrest of the Cell Cycle. To determine whether YC-1-induced growth inhibition was a cytotoxic or a cytostatic effect, we measured cell viability by trypan blue exclusion tests. It was shown that YC-1 (50 μM) did not significantly induce cell death in a 48-h treatment (mean ± SD = 6.8±2.2% for YC-1 samples; 5.8±1.9% for control samples, n = 4). By comparison, 3 μM doxorubicin, a reference chemotherapeutic drug, caused a dramatic 61.5±6.2% rate of cell death (n = 4). Additionally, YC-1 at a concentration of 50 μM did not induce a significant LDH release in HA22T cells (3.6±1.1% compared with control of 2.8±1.2%, n = 3). We examined apoptosis-induced nuclear morphology using DAPI staining and found that doxorubicin but not YC-1 induced a strong positive staining of condensed chromatin in nuclei, indicating a pro-apoptotic effect of doxorubicin (Fig. 2). Taken together, these data suggest that the YC-1-induced antiproliferative effect is not through direct cytotoxicity, but through the inhibition of cell growth. To further delineate the inhibitory mechanism of YC-1, cell cycle progression was

JPET Fast Forward. Published on November 3, 2004 as DOI: 10.1124/jpet.104.077230
This article has not been copyedited and formatted. The final version may differ from this version.

examined using FACScan flow cytometric analysis. As shown in Fig. 2D, YC-1 in the 10-100 μM range induced a concentration-dependent increase in the proportion of cells in G1 phase with a concomitant decrease in the number of cells in S and G2-M phases. These data support the notion that the G1 arrest of the cell cycle may be the basis for the antiproliferative effect of YC-1 on HA22T cells.

The YC-1-Induced Antiproliferative Effect is a cGMP-independent pathway. Because YC-1 has been shown to mediate numerous pharmacological effects through a cGMP-dependent pathway (Wu et al., 1995; Mulsch et al., 1997; Pan et al., 2004), we studied the role of cGMP in YC-1-induced growth inhibition in HA22T cells. As shown in Fig. 3, ODQ (a selective sGC inhibitor), and KT-5823 (a selective inhibitor of cGMP-dependent protein kinase) did not prevent the inhibition of cell growth that was induced by 50 μM YC-1. Moreover, intracelluar cGMP levels were also determined in this study (Table. 1). SNP (an NO donor), IBMX (an non-specific phosphodiesterase inhibitor), and YC-1 alone did not significantly increase the amount of cGMP in HA22T cells. SNP (100 μM) or IBMX (100 μM) combined with YC-1 (30 μM) also did not have a significant increase in cGMP levels. Neither the higher concentrations of SNP (300-1000 μM) nor IBMX (300-1000 μM) enhance YC-1 to increase cGMP levels in HA22T cells (data not shown). Taken together, these data suggest that the sGC/cGMP signaling pathway is not involved in YC-1-induced inhibition of HA22T proliferation.

JPET Fast Forward. Published on November 3, 2004 as DOI: 10.1124/jpet.104.077230
This article has not been copyedited and formatted. The final version may differ from this version.

Effect of YC-1 on the Phosphorylation of p42/p44 MAPK and Akt. Previous evidence suggests that the p42/p44 MAPK and PI3-Kinase signaling pathways play a crucial role in cell proliferation and survival (Graves et al., 1995; Brazil and Hemmings, 2001). We examined the effect of YC-1 on serum-induced activation of p42/p44 MAPK and Akt. As shown in Fig. 4, serum induced a significant increase in the phosphorylation of p42/p44 MAPK and Akt, while PD98059 (a selective MEK inhibitor) and LY294002 (a selective PI3-kinase inhibitor) almost completely abolished these serum-induced effects. YC-1 did not affect the phosphorylation or the expression of these two protein molecules (Fig. 4), suggesting that p42/p44 MAPK and PI3-Kinase pathways are not involved in YC-1's antiproliferative effect.

Effect of YC-1 on the Expression of G1-S Transition. In present study, YC-1 induced the G1 arrest of the cell cycle. We next investigated the effect of YC-1 on proteins involved in the G1 to S transition. As illustrated in Fig. 5A, 50 and 100 μM YC-1 did not significantly change the levels of cyclin D1 and E, nor did it modify the expression of CDK2 and 4 proteins (Fig. 5B). However, YC-1 did induce a profound elevation in $p21^{CIP1/WAF1}$ expression and a modest increase in $p27^{KIP1}$ levels after a 12-h application (data not shown). YC-1 increased $p21^{CIP1/WAF1}$ protein levels in a concentration-dependent manner (Fig. 5C). Quantitative densitometry showed that YC-1 (100 μM) induced 3.1±0.7 fold and 1.3±0.3 fold increases in $p21^{CIP1/WAF1}$ and $p27^{KIP1}$ expression, respectively. Since CKI induction normally

JPET Fast Forward. Published on November 3, 2004 as DOI: 10.1124/jpet.104.077230
This article has not been copyedited and formatted. The final version may differ from this version.

leads to an increase in binding and subsequent inactivation of the CDK-cyclin complex (Harper and Elledge, 1996), immunoprecipitation was carried out to examine the effect of YC-1 on the formation of the CDK-CKI complex. As shown in Fig. 6A, YC-1 significantly increased the binding of $p21^{CIP1/WAF1}$, but not $p27^{KIP1}$, to CDK2. The binding of $p21^{CIP1/WAF1}$ or $p27^{KIP1}$ to CDK4, on the other hand, was not increased by YC-1 (Fig. 6B). This suggests that the up-regulation of $p21^{CIP1/WAF1}$ and its association with CDK2 play a major role in the YC-1-induced G1 arrest in HA22T cells.

Antitumor Activity of YC-1 on HA22T Tumor Xenografts. On the basis of YC-1's potent antiproliferative effect *in vitro*, we investigated whether YC-1 possessed antitumor activities *in vivo*. We established xenografts with HA22T cells in athymic SCID mice, as tumors reached 60 mm^3 in size, mice were divided into four groups and orally treated with vehicle or YC-1. As shown in Fig. 7A, YC-1 induced a dose-dependent inhibition of tumor growth (YC-1 10 mg/kg, 282±68 mm^3 , $p < 0.05$; YC-1 30 mg/kg, 215±34 mm^3 , $p < 0.01$; YC-1 100 mg/kg, 143±23 mm^3 , $p < 0.001$ verus vehicle ; vehicle-treated group = 561±81 mm^3 on day 84), indicating the *in vivo* efficacy of orally administered YC-1. Tumors were removed on day 84, the weights of tumors from YC-1-treated grpups were also smaller than vehicle-treated group (Fig. 7B). Furthermore, we observed little difference in body weights between control and YC-1-treated animals (data not shown), indicating that YC-1 produced minimal toxicity *in vivo*.

JPET Fast Forward. Published on November 3, 2004 as DOI: 10.1124/jpet.104.077230
This article has not been copyedited and formatted. The final version may differ from this version.

YC-1's Cytostatic Effect and Cell Cycle-regulated Proteins in HA22T Xenografts. To investigate the *in vivo* antitumor mechanism of YC-1, several markers of proliferation and CKI proteins were evaluated. An anti-Ki-67 antibody was used as a biomarker of proliferation. YC-1 induced a significant reduction in positive staining cells, confirming the *in vivo* antiproliferative effect of YC-1 (Fig. 8B). We then evaluated two CKIs, $p21^{CIP1/WAF1}$ and $p27^{KIP1}$. As illustrated in Fig. 8C, basal levels of $p21^{CIP1/WAF1}$ protein were detected in nuclei of the vehicle-treated group. Moreover, the level of $p21^{CIP1/WAF1}$ was significantly increased by YC-1 (Fig. 8D). Interestingly, $p27^{KIP1}$ protein immunoreactivity was detected in the cytosol (Fig. 8E), and the level of $p27^{KIP1}$ was not affected by YC-1 (Fig. 8F). The opposite effects of YC-1 on Ki-67 (Fig. 8G) and $p21^{CIP1/WAF1}$ (Fig. 8H) expression suggest that the YC-1-induced antiproliferative effect *in vivo* may result from an increase in $p21^{CIP1/WAF1}$ expression.

JPET Fast Forward. Published on November 3, 2004 as DOI: 10.1124/jpet.104.077230
This article has not been copyedited and formatted. The final version may differ from this version.

Discussion

In the present study, we have shown that YC-1 induced an antiproliferative effect in HCC cells in a concentration-dependent manner. YC-1 also inhibited DNA synthesis in HA22T cells and blocked the G1-S transition of the cell cycle. It is well known that elevation of the cGMP levels can be achieved by YC-1 through direct activation of sGC (Wu et al., 1995) and by inhibition of phosphodiesterase activity (Galle et al., 1999). Nevertheless, YC-1-mediated responses through a cGMP-independent pathway have also been described before (Ferrero and Torres, 2001; Hwang et al., 2003). In our study, ODQ (a selective sGC inhibitor) and KT-5823 (a selective inhibitor of cGMP-dependent protein kinase) did not prevent the YC-1-induced antiproliferative effect, nor did YC-1 increase cGMP formation in HA22T cells. These results suggest that YC-1-induced inhibition of HA22T proliferation occurs through a cGMP independent signaling pathway. Soluble guanylyl cyclase is a haem-containing protein found in the cytosolic fraction of virtually all mammalian cells, with the high concentrations found in lung and brain, and the lower amounts detected in liver (Hobbs, 1997). Furthermore, the activity of sGC in hepatoma is less than in normal liver (Kimura and Murad, 1975). Therefore, we suggest that human HCC cells seem to be lack of sGC so that can not get the response-triggered from YC-1 to exert a cGMP signaling pathway.

Mitogen-dependent progression through the first gap phase (G1) and initiation of DNA

JPET Fast Forward. Published on November 3, 2004 as DOI: 10.1124/jpet.104.077230
This article has not been copyedited and formatted. The final version may differ from this version.

synthesis (S phase) during the mammalian cell division cycle are co-regulated by several classes of CDKs, positive cofactor-cyclins, and negative cofactor-CDK inhibitors (CKIs) (Lundberg and Weinberg, 1999). In the current study, YC-1 induced G1 arrest of the cell cycle in HA22T cells, given that CDK4/6-cyclin D1 complexes are involved in early G1 phase, and transition from G1 to S is regulated by the CDK2-cyclin E complex. The proteins which regulate the progression of G1 phase and transition to S phase, were measured after YC-1 treatment. We found that YC-1 did not induce significant changes in the expression of cyclin D1, cyclin E, CDK2, or CDK4 in HA22T cells. Instead, YC-1 stimulated a profound increase of $p21^{CIP1/WAP1}$, and a modest increase of $p27^{KIP1}$. It has been well-established that CKIs bind and inactivate CDK-cyclin complexes, in which $p21^{CIP1/WAP1}$ and $p27^{KIP1}$ are related proteins with a preference for CDK2- and CDK4-cyclin complexes (Sherr and Roberts, 1995). Our data indicated that the formation of CDK2-p21 complexes, but not other CDK-CKI complexes, was increased by YC-1. Taken together, the up-regulation of $p21^{CIP1/WAP1}$ CKI and its association with CDK2 explains the YC-1-induced G1 arrest in HA22T cells.

Loss of $p27^{KIP1}$ expression has been reported in a number of human tumor types including HCC, and is associated with poor prognosis and tumor aggressiveness (Chetty, 2003). In normal cells, $p27^{KIP1}$ is localized in the nucleus, where it binds to and inhibits CDK2, an activator of E2F1, and promotes DNA replication (Sherr and Roberts, 1995). In certain

JPET Fast Forward. Published on November 3, 2004 as DOI: 10.1124/jpet.104.077230
This article has not been copyedited and formatted. The final version may differ from this version.

carcinomas (e.g. breast, esophagus, and colon), $p27^{KIP1}$ is sequestered in the cytoplasm (Blain and Massague, 2002). In this situation, CDK2 is not inhibited by $p27^{KIP1}$ and freely activates E2F1, resulting in cell cycle progression and tumorigenesis. Recently, several groups demonstrated that $p27^{KIP1}$ phosphorylation by the oncogenically activated kinase AKT/PKB contributed to the impairment of $p27^{KIP1}$ nuclear import and subsequent cytoplasmic sequestration (Blain and Massague, 2002; Viglietto et al., 2002). In our study, we observed cytoplasmic dislocation of $p27^{KIP1}$ in HA22T cells in a xenografted tumor. YC-1 did not promote nuclear localization of $p27^{KIP1}$ *in vivo*, increase $p27^{KIP1}$ binding to CDK2 or CDK4 *in vitro*, or inhibit serum-induced phosphorylation of AKT in HA22T cells. The over-regulation of the PI3K/PKB signaling pathway in HA22T cells may disturb the nuclear localization signal of $p27^{KIP1}$. Although YC-1 induces the expression of $p27^{KIP1}$, it cannot enter into the nucleus to exert its function.

Parallel *in vivo* studies were carried out to confirm YC-1's antitumor effects. Subcutaneous xenografts of HA22T cells were established in athymic SCID mice. In control animals, the tumors grew slowly in the first two months after cell inoculation but rapidly thereafter. Orally administered YC-1 produced a dose-dependent inhibition of tumor growth, indicating its *in vivo* efficacy. Little toxicity was seen with YC-1 treatment (lack of body weight reduction). The tumor tissues were also examined with a Ki-67 biomarker, which is expressed in the nuclei of continuously cycling cells in late G1, S, M and G2 phases, but not in G0 phase

JPET Fast Forward. Published on November 3, 2004 as DOI: 10.1124/jpet.104.077230
This article has not been copyedited and formatted. The final version may differ from this version.

(Scholzen and Gerdes, 2000). Immunohistochemical analyses revealed intensive Ki-67-positive staining in control tumors, indicating a sustained induction of cell proliferation. In constrast, YC-1 caused a profound inhibition of cell proliferation, in which significantly less Ki-67 staining was detected. A dramatic increase in $p21^{CIP1/WAP1}$ protein was also noted in the nuclei of YC-1-treated regressed tumor tissue. These findings are consistent with previous *in vitro* studies and suggest that the induction of $p21^{CIP1/WAP1}$ up-regulation may primarily contribute to YC-1-mediated inhibition of HA22T tumor growth *in vivo*.

In human cancer cells, both intratumoral hypoxia and genetic alterations affecting signal transduction increase the level of hypoxia-inducible factor-1 (HIF-1), which promotes angiogenesis, metastasis, and tumor progression (Semenza, 2003). HIF-1α is subject to rapid ubiquitination and proteasomal degradation under non-hypoxic conditions; this process is inhibited under hypoxic conditions (Sutter, 2000). Stimulation of cells by growth factors, such as epidermal growth factor, fibroblast growth factor, and insulin-like growth factor, induces the expression and DNA-binding activity of HIF-1α protein and expression of its target genes under non-hypoxic conditions (Semenza, 2003). These ligands bind with their cognate receptor tyrosine kinase and activate a variety of pathways, including PI3-kinase/Akt and p42/p44 MAPK signaling (Richard et al., 1999; Zhong et al., 2000). It has been suggested that YC-1 can inhibit HIF-1 activity (Yeo et al., 2003). In our study, even high concentrations of YC-1 did not modify the phosphorylation of p42/p44 MAPK and Akt,

JPET Fast Forward. Published on November 3, 2004 as DOI: 10.1124/jpet.104.077230
This article has not been copyedited and formatted. The final version may differ from this version.

suggesting that p42/p44 MAPK and PI3-Kinase/Akt signaling pathways are probably not involved in YC-1's antiproliferative effect. Therefore, HIF-1 does not appear to play a major role in YC-1-mediated effects on HA22T, although we could not exclude its contribution either.

This study is the first to demonstrate that YC-1 directly inhibits proliferation of cancer cells. On the basis of our findings, we conclude that YC-1 induces cell cycle arrest and inhibits tumor growth both *in vitro* and *in vivo* via the up-regulation of $p21^{CIP1/WAP1}$ expression. Thus, YC-1 may produce multiple effects that inhibit tumor growth *in vivo*, including directly inhibiting the proliferation of cancer cells and suppressing HIF-1's activity which is expressed in tumors and renders cells. As a cytostatic agent, YC-1 slows the proliferation of cancer cells, while causing low toxicity to normal cells and allowing patients to "live with their cancer". Used alone or in combination with other chemotherapeutic agents, YC-1 deserves further investigation in preclinical studies or clinical trial as a potential antitumor agent.

References

Blain SW and Massague J (2002) Breast cancer banishes p27 from nucleus. *Nat Med* **8:**1076-1078.

Brazil DP and Hemmings BA (2001) Ten years of protein kinase B signalling: a hard Akt to follow. *Trends Biochem Sci* **26:**657-664.

Chetty R (2003) p27 Protein and cancers of the gastrointestinal tract and liver: an overview. *J Clin Gastroenterol* **37:**23-27.

Elledge SJ (1996) Cell cycle checkpoints: preventing an identity crisis. *Science* **274:**1664-1672.

El-Serag HB (2002) Hepatocellular carcinoma: an epidemiologic view. *J Clin Gastroenterol* **35:**S72-78.

El-Serag HB and Mason AC (1999) Rising incidence of hepatocellular carcinoma in the United States. *N Engl J Med* **340:**745-750.

Ferrero R and Torres M (2001) Prolonged exposure to YC-1 induces apoptosis in adrenomedullary endothelial and chromaffin cells through a cGMP-independent mechanism. *Neuropharmacology* **41:**895-906.

Galle J, Zabel U, Hubner U, Hatzelmann A, Wagner B, Wanner C and Schmidt HH (1999) Effects of the soluble guanylyl cyclase activator, YC-1, on vascular tone, cyclic GMP levels and phosphodiesterase activity. *Br J Pharmacol* **127:**195-203.

Gibbs JB (2000) Mechanism-based target identification and drug discovery in cancer research. *Science* **287:**1969-1973.

Graves JD, Campbell JS and Krebs EG (1995) Protein serine/threonine kinases of the MAPK cascade. *Ann N Y Acad Sci* **766:**320-343.

Harper JW, and Elledge SJ (1996) Cdk inhibitors in development and cancer. *Curr Opin Genet Dev* **6:**56-64.

Harper JW, Elledge SJ, Keyomarsi K, Dynlacht B, Tsai LH, Zhang P, Dobrowolski S, Bai C, Connell-Crowley L, and Swindell E (1995) Inhibition of cyclin-dependent kinases by p21. *Mol Biol Cell* **6:**387-400.

Hobbs AJ (1997) Soluble guanylate cyclase: the forgotten sibling. *Trends Pharmacol Sci* **18:**484-491.

Hsu HK, Juan SH, Ho PY, Liang YC, Lin CH, Teng CM, and Lee WS (2003) YC-1 inhibits proliferation of human vascular endothelial cells through a cyclic GMP-independent pathway. *Biochem Pharmacol* **66:**263-271.

Hwang TL, Hung HW, Kao SH, Teng CM, Wu CC, and Cheng SJ (2003) Soluble guanylyl cyclase activator YC-1 inhibits human neutrophil functions through a cGMP-independent but cAMP-dependent pathway. *Mol Pharmacol* **64:**1419-1427.

Kimura H and Murad F (1975) Increased particulate and decreased soluble guanylate cyclase activity in regenerating liver, fetal liver, and hepatoma. *Proc Natl Acad Sci U S A*

72:1965-1969.

Lee MH, Reynisdottir I, and Massague J (1995) Cloning of p57KIP2, a cyclin-dependent kinase inhibitor with unique domain structure and tissue distribution. *Genes Dev* **9:**639-649.

Lundberg AS and Weinberg RA (1999) Control of the cell cycle and apoptosis. *Eur J Cancer* **35:**1886-1894.

Malumbres M and Barbacid M (2001) To cycle or not to cycle: a critical decision in cancer. *Nat Rev Cancer* **1:**222-231.

Millar AW and Lynch KP (2003) Rethinking clinical trials for cytostatic drugs. *Nat Rev Cancer* **3:**540-545.

Morgan DO (1995) Principles of CDK regulation. *Nature* **374:**131-134.

Mulsch A, Bauersachs J, Schafer A, Stasch JP, Kast R, and Busse R (1997) Effect of YC-1, an NO-independent, superoxide-sensitive stimulator of soluble guanylyl cyclase, on smooth muscle responsiveness to nitrovasodilators. *Br J Pharmacol* **120:**681-689

Owa T, Yoshino H, Yoshimatsu K, and Nagasu T (2001) Cell cycle regulation in the G1 phase: a promising target for the development of new chemotherapeutic anticancer agents. *Curr Med Chem* **8:**1487-1503.

Pan SL, Guh JH, Chang YL, Kuo SC, Lee FY, and Teng CM (2004) YC-1 prevents sodium nitroprusside-mediated apoptosis in vascular smooth muscle cells. *Cardiovasc Res* **61:**152-158.

Parkin DM, Pisani P, and Ferlay J (1999) Estimates of the worldwide incidence of 25 major cancers in 1990. *Int J Cancer* **80:**827-841.

Pines J (1991) Cyclins: wheels within wheels. *Cell Growth Differ* **2:**305-310.

Polyak K, Lee MH, Erdjument-Bromage H, Koff A, Roberts JM, Tempst P, and Massague J (1994) Cloning of p27Kip1, a cyclin-dependent kinase inhibitor and a potential mediator of extracellular antimitogenic signals. *Cell* **78:**59-66.

Richard DE, Berra E, Gothie E, Roux D and Pouyssegur J (1999) p42/p44 mitogen-activated protein kinases phosphorylate hypoxia-inducible factor 1alpha (HIF-1alpha) and enhance the transcriptional activity of HIF-1. *J Biol Chem* **274:**32631-32637.

Scholzen T and Gerdes J (2000) The Ki-67 protein: from the known and the unknown. *J Cell Physiol* **182:**311-322.

Semenza GL (2003) Targeting HIF-1 for cancer therapy. *Nat Rev Cancer* **3:** 721-732.

Sherr CJ (2000) The Pezcoller lecture: cancer cell cycles revisited. *Cancer Res* **60:** 3689-3695.

Sherr CJ and Roberts JM (1995) Inhibitors of mammalian G1 cyclin-dependent kinases. *Genes Dev* **9:**1149-1163.

Stewart ZA, Westfall MD, and Pietenpol JA (2003) Cell-cycle dysregulation and anticancer therapy. *Trends Pharmacol Sci* **24**:139-145.

Sutter CH, Laughner E and Semenza GL (2000) Hypoxia-inducible factor 1alpha protein

expression is controlled by oxygen-regulated ubiquitination that is disrupted by deletions and missense mutations. *Proc Natl Acad Sci U S A* **97:** 4748-4753.

Vidal A and Koff A (2000) Cell-cycle inhibitors: three families united by a common cause. *Gene* **247:**1-15.

Viglietto G, Motti ML, Bruni P, Melillo RM, D'Alessio A, Califano D, Vinci F, Chiappetta G, Tsichlis P, Bellacosa A, Fusco A and Santoro M (2002) Cytoplasmic relocalization and inhibition of the cyclin-dependent kinase inhibitor p27 (Kip1) by PKB/Akt-mediated phosphorylation in breast cancer. *Nat Med* **8:**1136-1144.

Wu CC, Ko FN, Kuo SC, Lee FY, and Teng CM (1995) YC-1 inhibited human platelet aggregation through NO-independent activation of soluble guanylate cyclase. *Br J Pharmacol* **116:**1973-1978.

Wu CH, Chang WC, Chang GY, Kuo SC, and Teng CM **(**2004) The inhibitory mechanism of YC-1, a benzyl indazole, on smooth muscle cell proliferation: an in vitro and in vivo study. *J Pharmacol Sci* **94:**252-260.

Yeo EJ, Chun YS, Cho YS, Kim J, Lee JC, Kim MS, and Park JW (2003) YC-1: a potential anticancer drug targeting hypoxia-inducible factor 1. *J Natl Cancer Inst* **95:**516-525.

Zhong H, Chiles K, Feldser D, Laughner E, Hanrahan C, Georgescu MM, Simons JW and Semenza GL (2000) Modulation of hypoxia-inducible factor 1alpha expression by the epidermal growth factor /phosphatidylinositol 3-kinase/ PTEN/AKT/FRAP pathway in

human prostate cancer cells: implications for tumor angiogenesis and therapeutics. *Cancer Res* **60:**1541-1545.

Footnotes.

Financial support: This work was supported by a research grant of the National Science Council of the Republic of China (NSC 92-2320-B-002-072).

JPET Fast Forward. Published on November 3, 2004 as DOI: 10.1124/jpet.104.077230
This article has not been copyedited and formatted. The final version may differ from this version.

Legends

Fig. 1. Effect of YC-1 on cell growth in human HCC cells. A, HA22T and Hep3B cells were treated with indicated concentration of YC-1 for 48 h in medium containing 10% FBS, and then the cell growth was detected by SRB assay as described under *Materials* and *Methods*. Data are expressed as means ± SEM of five determinations (each in triplicate). *, $p < 0.05$; ***, $p < 0.001$ compared with the control of HA22T cells. #, $p < 0.05$; ##, $p < 0.01$; ###, $p < 0.001$ compared with the control of Hep3B cells. B, HA22T cells were treated without or with indicated concentration of YC-1 for 48 h, and the detection of DNA synthesis was examined by [^{3}H]Thymidine incorporation as described under *Materials* and *Methods*. Data are expressed as means ± SEM of five determinations (each in triplicate). *, $p < 0.001$ compared with the basal. #, $p < 0.05$; ##, $p < 0.01$ compared with the control.

Fig. 2. Effect of YC-1 on apoptosis and cell cycle progression in HA22T cells. Cells were exposed to vehicle (A), YC-1 (50 μM, B), or doxorubicin (3 μM, C) for 24 hr. Then, the identification of apoptotic cell death was examined by DAPI staining as described under *Materials* and *Methods*. Furthermore, cells were treated with or without YC-1 for 24 h, and then the cells were harvested for the detection of cell cycle distribution using FACScan flow cytometric analysis (D) as described under *Materials* and *Methods*. The data are expressed as means ± SEM of three individual experiments.

JPET Fast Forward. Published on November 3, 2004 as DOI: 10.1124/jpet.104.077230
This article has not been copyedited and formatted. The final version may differ from this version.

Fig. 3. Effect of YC-1 on sGC/cGMP signaling pathway in HA22T cells. Cells were incubated without or with YC-1 (50 μM) and the indicated agent for 48 h. The cell growth was detected by SRB assay as described under *Materials* and *Methods*. Data are expressed as means ± SEM of five determinations (each in triplicate). *, $p < 0.01$ compared with the control. #, $p < 0.05$ compare with YC-1 alone.

Fig. 4. Effect of YC-1 on the expression of phosphorylated p42/p44 MAPK and Akt in HA22T cells. Cells were made quiescent for 48 h, and then vehicle (basal) or 10% FBS was added to the cells in the absence (control) or presence of YC-1 for 10 min. Cells were harvested for the detection of phosphorylated-p42/p44 MAPK and total p42/p44 MAPK (A), and phosphorylated-Akt and total Akt (B) using Western blot analysis as described under *Materials* and *Methods*. Blots were representative of results from three separate experiments.

Fig. 5. Effect of YC-1 on the expression of G1-S transition protein in HA22T cells. A, Cells were incubated without (control) or with YC-1 (50 and 100 μM) for the indicated times. B, Cells were incubated without (control) or with 50 μM YC-1 for the indicated time courses. C, Cells were incubated in the absence (control) or presence of YC-1 (10-100 μM) for 12 h. After the above treatment (A, B, and C), the cells were harvested and lysed for the detection of cyclin D1 and E (A) ; CDK2 and 4 (B) ; $p21^{CIP1/WAF1}$ and $p27^{KIP1}$ (C) protein expressions by Western blot analysis as described under *Materials* and *Methods*. Densitometric analysis for the relative level of $p21^{WAF1}$ and $p27^{KIP1}$ protein. Values are expressd as means ± SEM

JPET Fast Forward. Published on November 3, 2004 as DOI: 10.1124/jpet.104.077230
This article has not been copyedited and formatted. The final version may differ from this version.

(n=3). *, $p < 0.05$, **, $p < 0.01$, and ***, $p < 0.001$ compared with the control. Blots were representative of results from three separate experiments.

Fig. 6. Effect of YC-1 on $p21^{CIP1/WAF1}$ and $p27^{KIP1}$ association with CDK complexes in HA22T cells. Total cell lysates from cells treated with YC-1 (0-100 μM) for 12 h were used to immunoprecipate CDK2 complexes (A) and CDK4 complexes (B). Then, Western blots were performed to determine the association of $p21^{CIP1/WAF1}$ and $p27^{KIP1}$ with immunoprecipitated CDK complexes as described under *Materials* and *Methods*. Blots were representative of results from three separate experiments.

Fig. 7. Effect of YC-1 on antitumor activity in an *in vivo* model. HA22T cells were used to establish xenografts in athymic SCID mice, and tumor-bearing animals were treated on day 40. Animals (nine mice/group) were given vehicle (0.5% CMC, control), YC-1 (10, 30, 100 mg/kg/day) by oral treatment daily. A, The treatment period was indicated (day 40-84), and tumor volume was determined as described under *Materials* and *Methods*. Data are expressed as means of tumor volume (mm^3) ± SEM. B, Differences in tumor weights between control and YC-1-treated groups. Data are expressed as mean of tumor weight (g) ± SEM. *, $p < 0.05$ compared with the control.

Fig. 8. Effect of YC-1 on proliferation and CKI proteins in HA22T-xenografted tumors. HA22T tumor xenografts tissues from vehicle- (A, C, and E) and YC-1-treated (100 mg/kg/day) (B, D, and F) animals were obtained at the end of treatment period (day 84).

JPET Fast Forward. Published on November 3, 2004 as DOI: 10.1124/jpet.104.077230
This article has not been copyedited and formatted. The final version may differ from this version.

Ki-67 staining was performed for the detection of proliferating cells (A and B), and protein expressions of $p21^{CIP1/WAF1}$ (C and D) and $p27^{KIP1}$ (E and F) were detected using immunohistochemical analyses as described under *Materials* and *Methods*. The quantitative densitometry of Ki-67 (G) or $p21^{CIP1/WAF1}$ (H) protein expression was performed as described under *Materials* and *Methods*. Values are expressed as means ± SEM (n=5). *, $p < 0.05$; **, $p < 0.01$ compared with the control. The data are representative of three independent experiments.

JPET Fast Forward. Published on November 3, 2004 as DOI: 10.1124/jpet.104.077230
This article has not been copyedited and formatted. The final version may differ from this version.

Table.1 Effect of YC-1 on cGMP levels in HA22T cells

Treatment	cGMP (fmol/well)
Control	23.2 ± 4.0
YC-1 10 μM	25.5 ± 5.5
YC-1 30 μM	31.4 ± 6.4
YC-1 50 μM	33.6 ± 9.2
YC-1 100 μM	33.0 ± 8.3
SNP 100 μM	28.4 ± 2.3
SNP 300 μM	27.2 ± 0.8
YC-1 30 μM + SNP 100 μM	31.0 ± 1.8
IBMX 100 μM	27.5 ± 0.9
IBMX 300 μM	27.3 ± 0.9
YC-1 30 μM + IBMX 100 μM	32.3 ± 2.6

The data are expressed as mean ± SEM of five determinations (each in triplicate).

Table.1

JPET Fast Forward. Published on November 3, 2004 as DOI: 10.1124/jpet.104.077230
This article has not been copyedited and formatted. The final version may differ from this version.

Fig. 1

A.

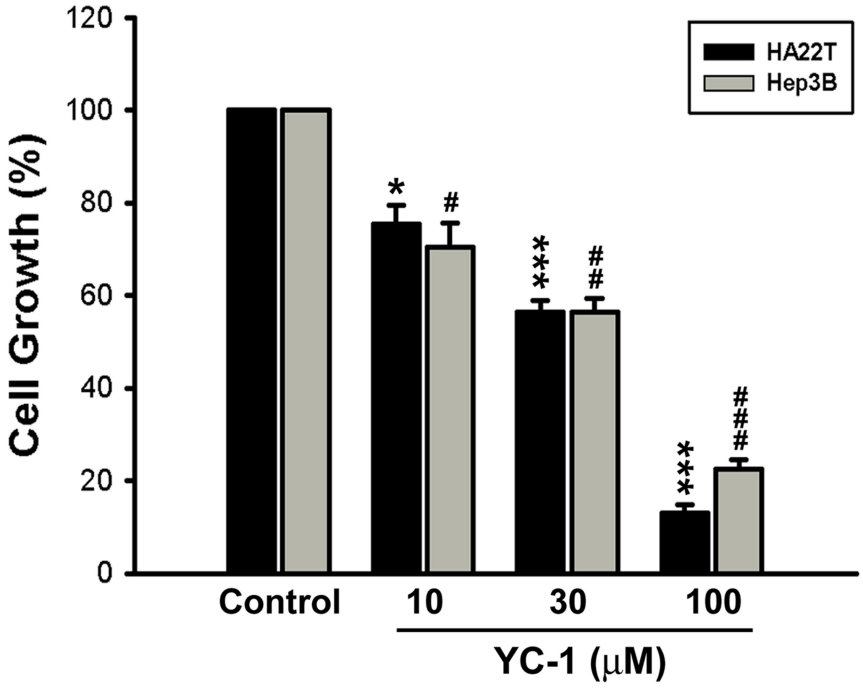

B.

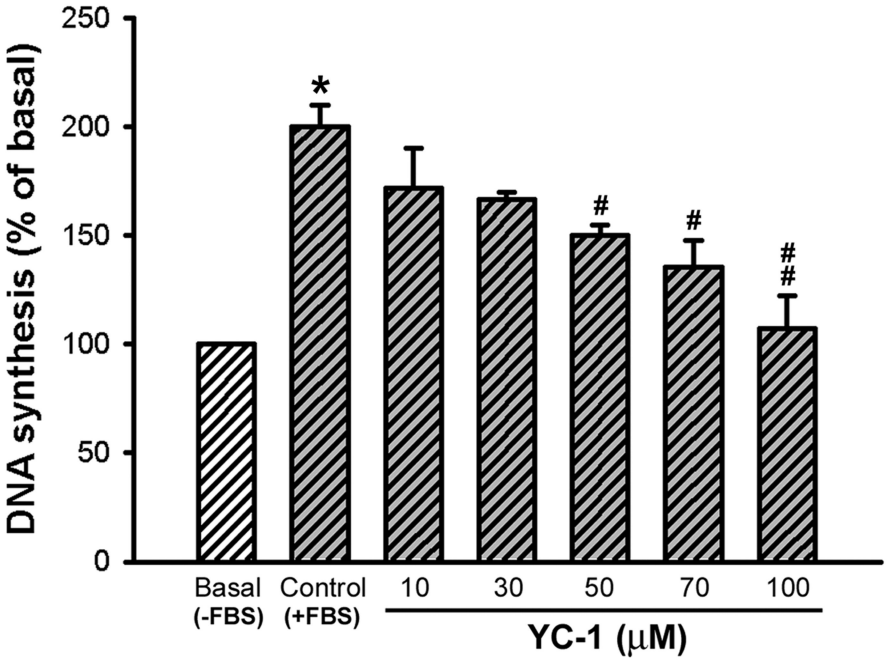

JPET Fast Forward. Published on November 3, 2004 as DOI: 10.1124/jpet.104.077230
This article has not been copyedited and formatted. The final version may differ from this version.

Fig. 2

A. B. C.

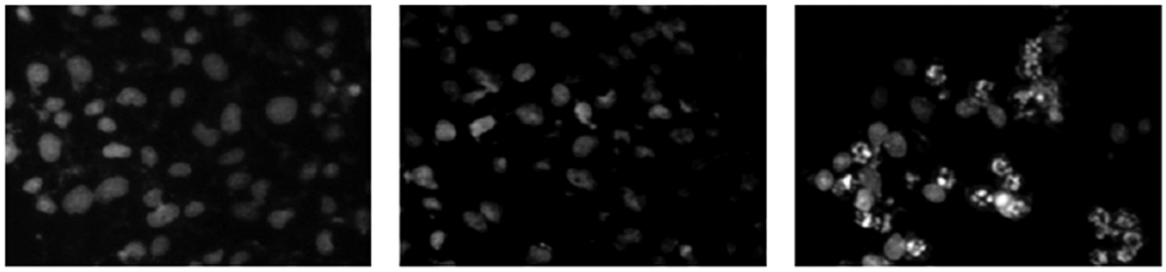

D.

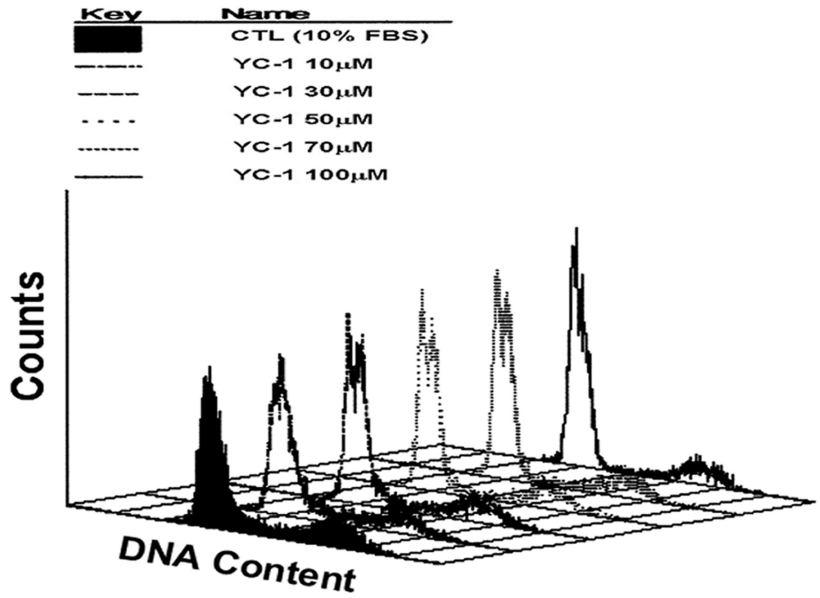

FACS (PI Staining)	Cell Cycle Distribution (%)			
	Sub-G1	G0/G1	S	G2/M
Control	1.0 ± 0.1	64.7 ± 4.4	11.3 ± 0.2	23.3 ± 4.4
YC-1 10 μM	1.8 ± 0.8	64.9 ± 0.2	10.5 ± 0.8	23.2 ± 0.1
YC-1 30 μM	1.8 ± 0.3	69.5 ± 1.5	8.0 ± 1.0	20.7 ± 1.2
YC-1 50 μM	2.1 ± 0.0	71.2 ± 0.8	7.0 ± 0.9	19.5 ± 0.5
YC-1 70 μM	2.0 ± 0.6	75.3 ± 2.8	7.5 ± 0.1	15.7 ± 3.1
YC-1 100 μM	2.7 ± 0.0	78.1 ± 1.1	7.4 ± 1.1	12.6 ± 0.6

JPET Fast Forward. Published on November 3, 2004 as DOI: 10.1124/jpet.104.077230

Fig. 3

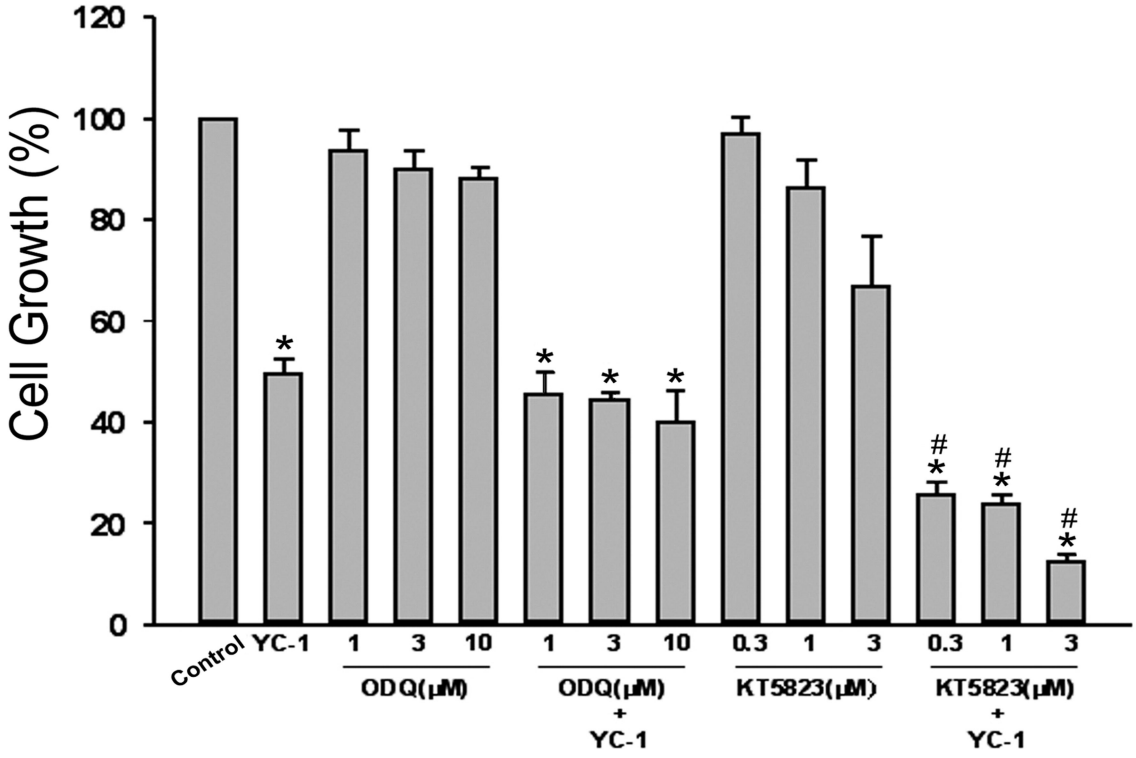

JPET Fast Forward. Published on November 3, 2004 as DOI: 10.1124/jpet.104.077230
This article has not been copyedited and formatted. The final version may differ from this version.

Fig. 4

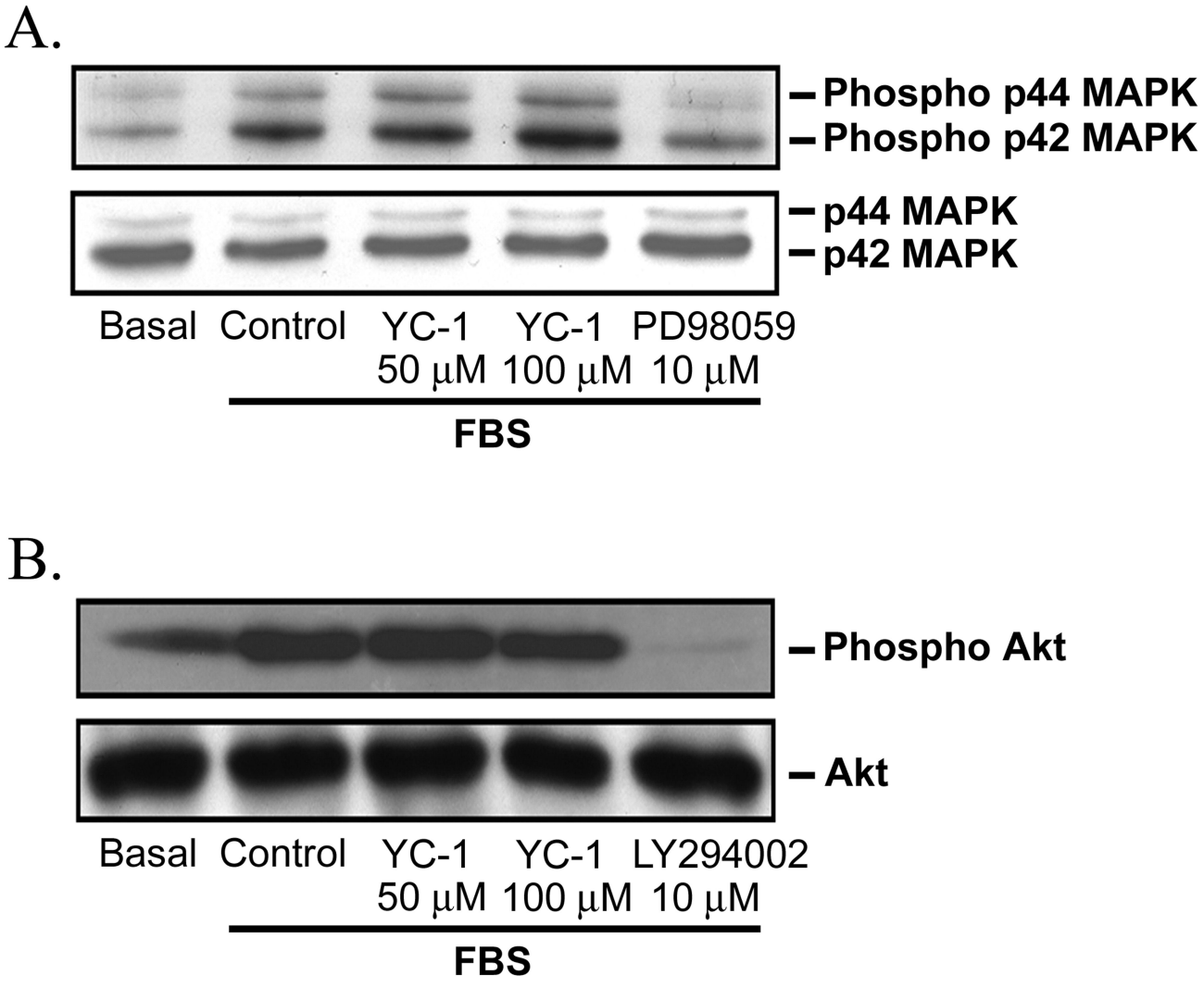

JPET Fast Forward. Published on November 3, 2004 as DOI: 10.1124/jpet.104.077230
This article has not been copyedited and formatted. The final version may differ from this version.

Fig. 5

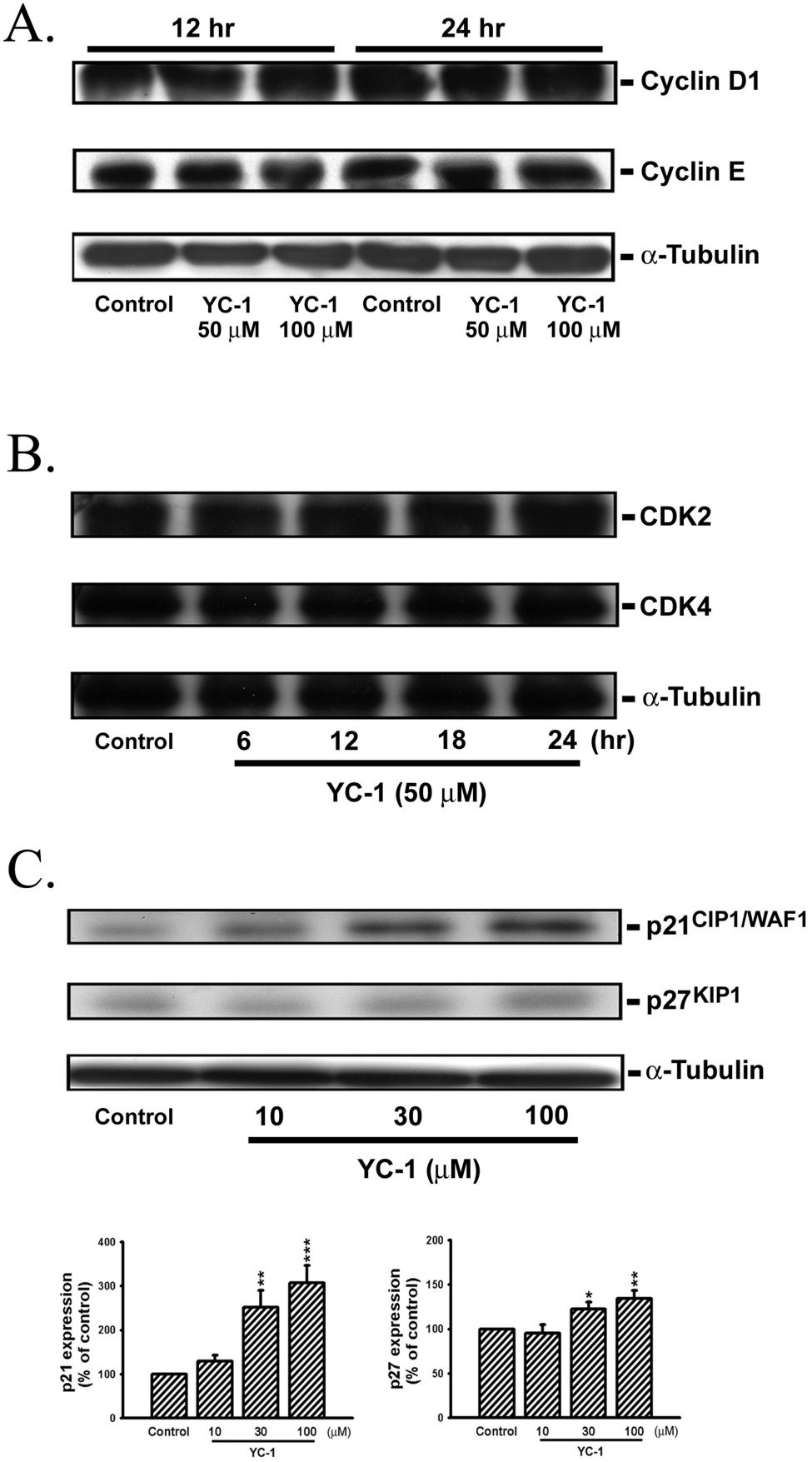

JPET Fast Forward. Published on November 3, 2004 as DOI: 10.1124/jpet.104.077230
This article has not been copyedited and formatted. The final version may differ from this version.

Fig. 6

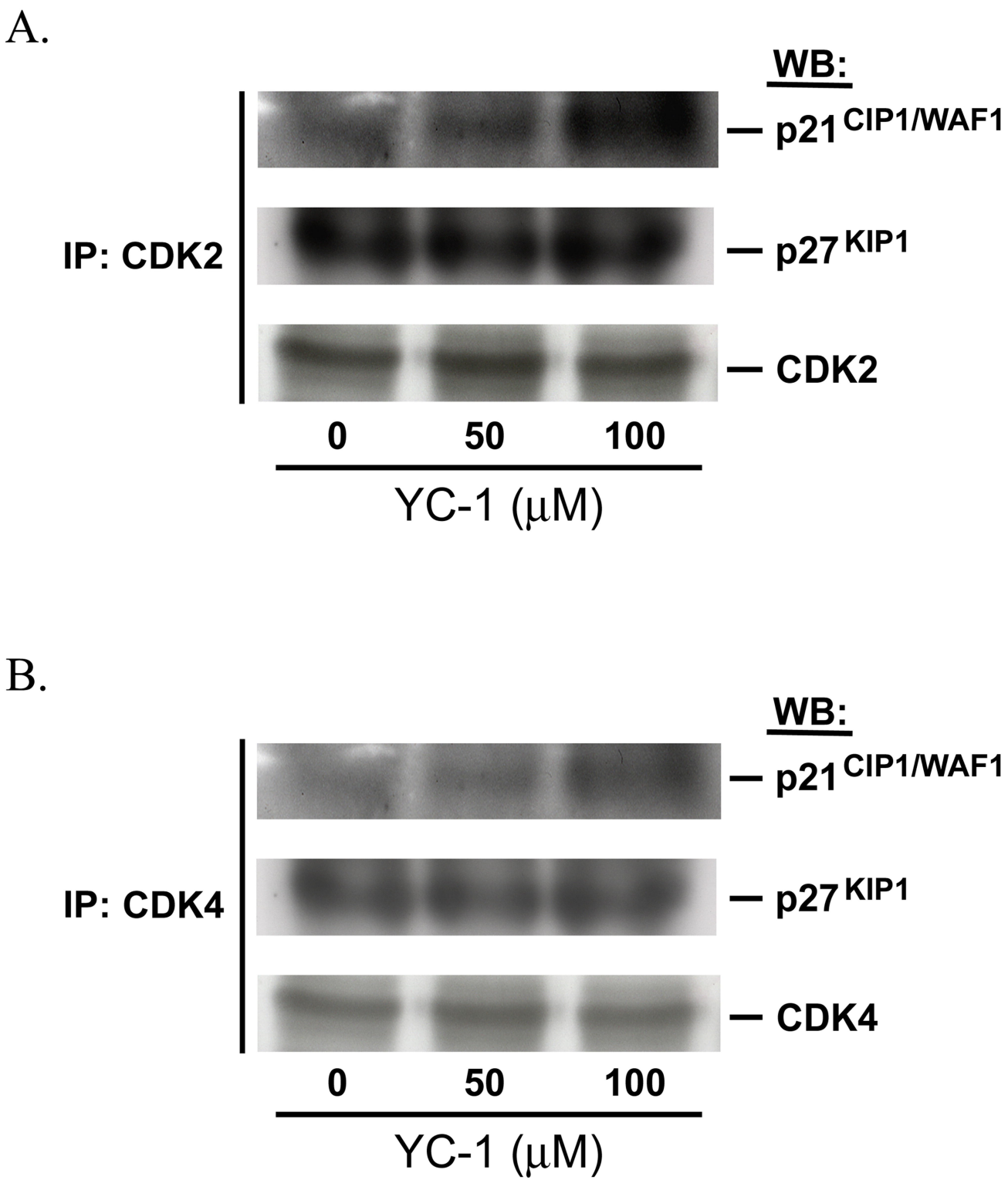

JPET Fast Forward. Published on November 3, 2004 as DOI: 10.1124/jpet.104.077230
This article has not been copyedited and formatted. The final version may differ from this version.

Fig. 7

A.

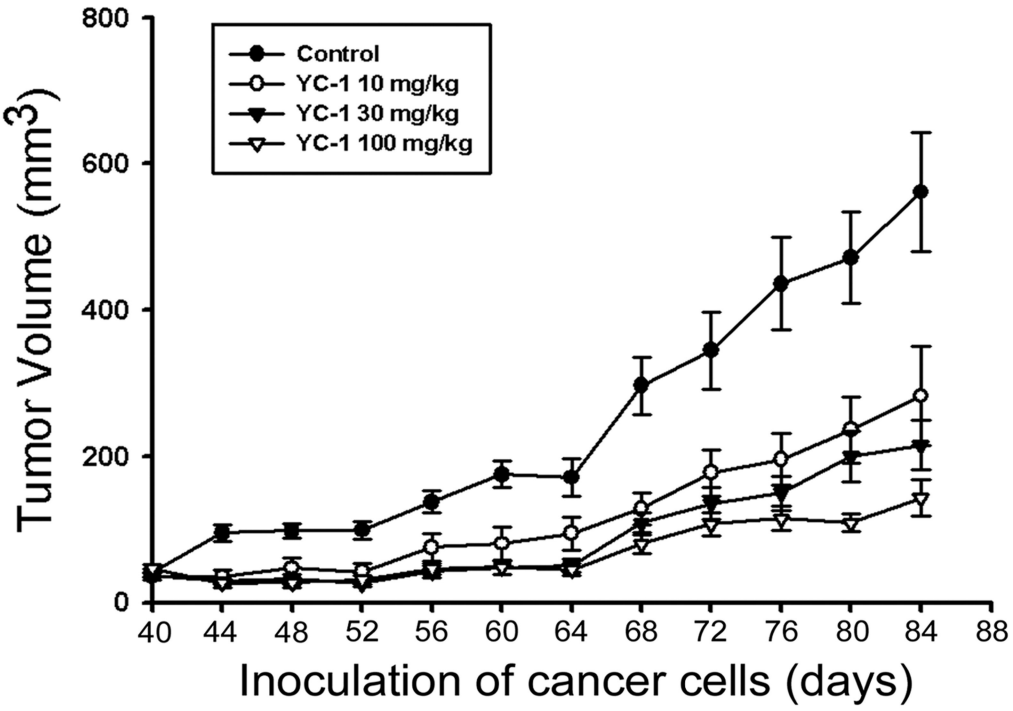

B.

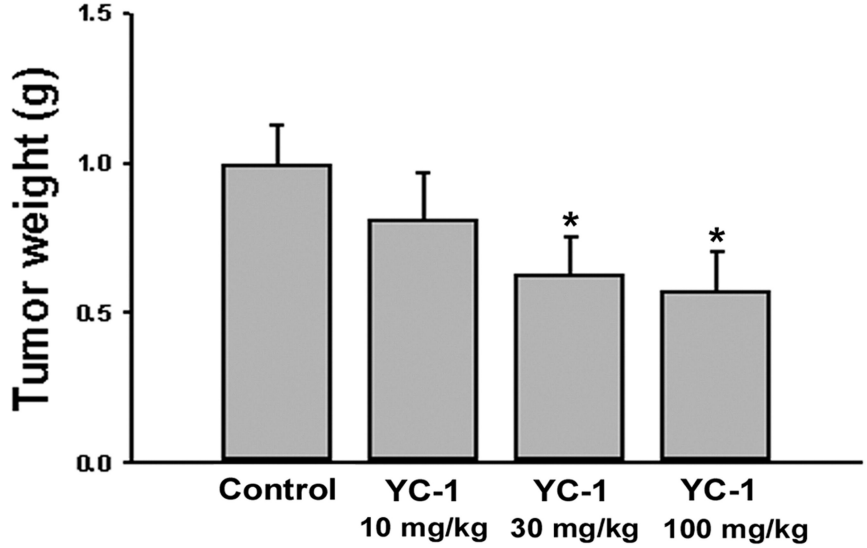

JPET Fast Forward. Published on November 3, 2004 as DOI: 10.1124/jpet.104.077230
This article has not been copyedited and formatted. The final version may differ from this version.

Fig. 8